High-resolution 3D marine seismic acquisition in the overburden at the Tomakomai CO_2 storage project, offshore Hokkaido, Japan

GCCC Publication Series #2019-9

T.A. Meckel

Y.E. Feng

R.H. Treviño

D. Sava

Keywords: 3D seismic, high-resolution, offshore, monitoring, Tomakomai, stratigraphy, above-zone, Moebetsu

Cited as:
Meckel, T.A., Feng, Y.E., Treviño, R.H., Sava, D., 2019, High-resolution 3D marine seismic acquisition in the overburden at the Tomakomai CO_2 storage project, offshore Hokkaido, Japan, GCCC Publication Series #2019-9.

High-resolution 3D marine seismic acquisition in the overburden at the Tomakomai CO_2 storage project, offshore Hokkaido, Japan

T.A. Meckel[1], Y.E. Feng[1], R.H. Trevino[1], D. Sava[1]

[1] Gulf Coast Carbon Center, Bureau of Economic Geology, Jackson School of Geosciences, The University of Texas at Austin, Austin, TX, USA

Corresponding author: Tip Meckel (tip.meckel@beg.utexas.edu)

Abstract

Monitoring injected CO_2 is an important part of assuring permanence of long term storage to mitigate atmospheric emissions. Three-dimensional (3D) seismic has been shown to be an effective technology for visualizing and quantifying subsurface geology and fluids. In this study, we demonstrate the successful acquisition, processing, and initial interpretation of a first-of-its-kind high-resolution 3D (HR3D) marine seismic survey above an active CO_2 injection site offshore Tomakomai, Japan. An initial sensitivity study indicated generally favourable subsurface conditions for imaging subsurface pore fluid changes. A unique processing workflow incorporating multiple data processing software packages has been tailored to the short-offset and low-fold HR3D acquisition. The final 3D volume shows generally flat and laterally-continuous stratigraphy in the overburden above the injection zone without identifiable faults, indicating coherent overburden above the CO_2 injection site and low associated risk of vertical CO_2 migration. The successful deployment of this novel marine seismic monitoring technology in the overburden at a small-scale (100 kt/yr) demonstration project suggests HR3D will also be a useful characterization and monitoring tool for larger demonstration and commercial-scale (~10 MT) offshore Carbon Capture and Storage (CCS) sites.

Keywords: Carbon Capture and Storage (CCS); High-resolution 3D seismic; CO_2 seismic monitoring; Tomakomai; Japan; Offshore; Overburden

Highlights:

- Successful demonstration of first HR3D seismic acquisition at an active offshore CCS site.
- Novel processing workflow incorporating multiple data processing software packages.
- Continuous 3D overburden characterization in high resolution.

1. Introduction

The Tomakomai CO_2 project is being undertaken as the first integrated industrial demonstration project of offshore CCS in Japan. The project goal is to demonstrate and verify the integrated CCS system, including CO_2 capture from hydrogen production offgas, compression and CO_2 injection and offshore storage (Tanaka et al., 2014). The Tomakomai injection site (Tanaka et al., 2017) has an impressive existing array of deployed monitoring technologies, which include a permanent ocean bottom cable (Ikeda and Tsuji, 2015), gravimetry (Shugihara et al., 2017), seafloor sediment and water column analyses, multiple permanent ocean-bottom seismometers, instrumentation in deep monitoring wells (Tanase and Tanaka, 2018), and conventional 3D seismic using temporary seafloor cable receiver arrays, which have NRMS seismic anomalies identified in the injection interval (Tanase and Tanaka, 2018).

HR3D uses closely spaced, short-offset streamers with small group intervals to achieve high lateral resolution of typically the upper kilometre of stratigraphy (Brookshire et al., 2016, Meckel and Mulcahy, 2017, Lebedeva-Inanova et al., 2018). Recording of high-frequency energy allows for meter-scale vertical resolution in the overburden. As the first application of marine HR3D seismic technology for CCS monitoring over an active injection site, the goal of the HR3D deployment is to complement the other various deployed geophysical monitoring techniques and validate HR3D technology for CCS projects in the following ways: 1) evaluate expected seismic sensitivity to CO_2 saturation in the subsurface, 2) map the geologic overburden above the injection interval in high resolution; 3) attempt to image CO_2 injected into the storage reservoir at approximately 1,100 meters below the seafloor; and 4) evaluate repeatability to inform capabilities for time-lapse monitoring studies comparing multiple HR3D acquisitions.

The HR3D survey was planned with cooperation from Japan CCS Co., Ltd. (JCCS) and the Japan Ministry of Economy, Trade and Industry (METI), and implemented as a collaboration between JGI, Inc. (JGI) and the Gulf Coast Carbon Center (GCCC; The University of Texas at Austin) as a part of the cooperative projects on CCS technologies, based on the Memorandum of

Cooperation signed on April 27, 2015 between US Department of Energy (DOE) and METI. JCCS submitted the seismic survey permission application and carried out the survey communication to Tomakomai Federation of Fisheries Cooperative Associations and others prior to acquisition. JGI and GCCC appreciate METI and JCCS for allowing for the opportunity to collect HR3D data at the Tomakomai CCS monitoring site.

After calculating the expected subsurface seismic response to variable CO_2 pore saturation, a 3 km^2 HR3D dataset was acquired over the injection site. The survey location is 1 to 4 km offshore Tomakomai City in Hokkaido with water depth of 10 to 35 m (Figure 1). At the time of the HR3D survey in August 2017, approximately 60,000 tonnes of CO_2 had been injected into the Moebetsu Formation at approximately 1,100 meters below the seafloor. We present a data processing workflow involving multiple processing software packages, which addresses the unique aspects of HR3D data. We discuss the detailed depositional stratigraphic features and coherent overburden stratigraphy that can be seen from the final HR3D volume, which are otherwise un-imaged in conventional 3D data. This improvement in shallow imaging will inform potential risks related to vertical CO_2 migration, especially in the un-imaged overburden section. These results document the successful implementation HR3D at an active offshore CCS site and validate HR3D as an appropriate and useful for characterization and monitoring.

2. Methodology

The major difference of HR3D survey compared to the conventional 3D surveys is the acquisition geometry – relatively short streamers and wide azimuth. Unlike the long streamers and deep imaging of conventional 3D surveys, the short streamer HR3D only allows imaging of the upper kilometer stratigraphy. However, this unique design provides extraordinary spatial resolution of the shallow interval. In this paper, we discuss the benefits and weakness of the HR3D survey and demonstrate our methods to overcome the weaknesses during data acquisition and processing.

2.1. Sensitivity

Prior to acquisition of the HR3D dataset, a standard theoretical sensitivity study was completed using well log data from the Tomakomai site to determine the anticipated seismic response of the injection interval (Moebetsu Formation) related to the changing subsurface pore fluid composition. At the injection interval depth of ~1,100 m, the Moebetsu formation can be

characterized as a high porosity sandstone (~28%) with low velocity (~2030 m/s Vp and ~593 m/s Vs). These conditions are generally favorable for seismic response related to changes in pore fluid composition. Similar sensitivity analyses have not been done for the entire overburden due to the typical lack of rock property data beyond the reservoir interval, but reservoir results are considered qualitatively representative of how similarly porous clastic material in the overburden might respond. In particular, shallower intervals are likely to be more responsive than the deeper injection interval due to decreased compaction and porosity reduction.

The quantitative seismic response to changes in saturation are understood through rock physics theories for elastic properties of porous media partially saturated with various fluids. The approach taken here is similar to that used by Vera and Lawton (2010) for the Paskapoo Formation in Alberta, Canada, but many other comparable examples exist. The seismic attributes considered here are the P-wave velocity (Vp) and the Acoustic Impedance (product between Vp and bulk density, or P-impedance, Ip).

Gassmann (1951) theory is used to predict seismic velocities for different CO_2 saturation conditions (Smith et al., 2003). The elastic properties needed for fluid sensitivity analysis for the Moebetsu are presented in Table 1. P and S-wave velocities and bulk density were extracted from well-log data (not presented here for brevity). Porosity is obtained from published core analysis (Ito et al., 2013). Mineral analysis of Moebetsu Formation cores show presence of four main components: plagioclase 36%, clay minerals 34.5%, quartz 16%, and K-feldspar 6.5%. Using Hashin-Shtrikman (1963) bounds and average properties of bulk modulus for these minerals from Mavko et al. (2003), the value for the bulk modulus of the mineral composite is calculated to be 40.9 GPa. The in situ conditions at ~1100 m are (Ito et al., 2013): brine salinity is 18000 ppm, average fluid pressure is 10.67 MPa, and temperature is 44.8 C. The in-situ elastic properties of the three fluid phases, brine CO_2, and the residual gas are presented in Table 1, as determined using relations in Han et al. (2010) and Batzle and Wang (1992).

When CO_2 displaces brine to occupy pore space, there are at least two fluid phases present in the porous space. Both homogeneous and patchy saturation assumptions are considered for the mixing of the CO_2 with the existing fluid in the pores. Reuss (1929) average is used to determine the bulk modulus of the fluid mixture for the homogeneous saturation. For the patchy saturation the volumetric average for the bulk modulus and density of the fluid phases is used.

Calculations indicate that P-wave velocity and P-impedance both decrease with increasing CO_2 saturation in pores (Figure 2), as expected from much prior theoretical and applied work. At seismic wavelengths the assumption of homogeneous saturation may be more representative of how the fluids are mixed in the subsurface. In Figure 2, the line at -5% velocity reduction in velocity represents a conservative limit of seismic detectability, such that changes larger than 5% are expected to be seismically observable (Xue and Ohsumi, 2004). The assumption of fine-scale mixing, modeled using Reuss average, predicts that just a few percentages of CO_2 present in the pores can significantly affect the geophysical properties of the injection interval and may be seismically observable. Saturations would need to be above 20% for detectability if a patchy saturation model is accurate. Field data often plot between the two theoretical curves (Lumley, 2010). In summary, in the absence of residual methane (not modeled here), and with high-quality seismic data (high signal-to-noise ratio), the presence and distribution of CO_2 should be identifiable in the Moebetsu Formation using seismic methods. However, such seismic anomaly in the overburden may not be observable with a conventional 3D dataset. This further motivated the acquisition of HR3D data at the Tomakomai site.

2.2. HR3D data acquisition

Seismic acquisition components (streamers, recording system, acoustic source, etc.) were provided by the Gulf Coast Carbon Center (shipped from U.S.) and in-water, real-time GPS positioning was provided by JGI using ION's *Orca*® towed streamer navigation system. The *R/V Kaikō Maru No. 7* was utilized, having just finished acquiring a conventional temporary ocean-bottom cable seismic survey at the CO_2 injection site (Tanase and Tanaka, 2018). The Tomakomai HR3D survey was acquired using the configuration shown in Figure 3. The array design comprised four streamers of 25 m length with 10 m inline separation. Each solid-core Geometrics *GeoEel*^{TM} streamer has 8 channels (32 total array channels) with a 3.125 m group interval spacing, resulting in a remarkably small final processing bin size of 3 x 3 m. The wide azimuth range of such short offset streamers compared to the long offset conventional streamer setting may provide opportunities for azimuthal velocity analysis, though not undertaken here. Source and receiver positioning were achieved using five rGPS in-water units (*BuoyLink 4DX*) and a DGPS antennae on the vessel (*NetR9 GNSS* receiver series). A 210 cubic inch generator-injector (GI) *Sercel* airgun was used as an acoustic source, with air compression delivered from the dedicated on-board 2000

PSI compression unit. After four days of vessel mobilization and equipment testing, approximately three square kilometres of HR3D data (including repeated lines; Figure 1) were acquired over a period of five days during obligatory daylight operating hours. Because of the inherent low-fold resulting from short streamers, a decision was made during acquisition to conduct repeat passes for lines on the eastern side of the survey, closer to the bottom-hole location of the Moebetsu CO_2 injection well (Figure 1). Overall, 30 individual lines were collected. The NW part of the survey includes 12 lines with only primary passes, which resulted in inconsistent fold (data density; number of samples per bin) across the survey area, but increased fold and reduction of data gaps requiring interpolation directly over the Moebetsu injection area (Figure 4).

2.3. HR3D data processing workflow

Due to the short-offset streamers and low-fold coverage, HR3D brings unique challenges in seismic data processing which require a different data processing workflow tailored to the HR3D acquisition. Shot geometry and the resulting data are very sensitive to horizontal and vertical position accuracy. The GPS location and depth of both sources and receivers are of great significance in creating accurate seismic images, especially with relatively low-fold data that short streamers produce. In addition, swells and tidal levels can affect the relative positioning of the acquisition system, and may cause significant static issues on high resolution seismic data. Another challenge related to the short streamers and wide azimuth is the difficulty of establishing accurate subsurface interval velocities. Incorrect velocities can affect flatness of NMO gathers and produce inferior migration results.

In this study, we designed a unique processing workflow (Figure 5) which involves three commercial and one non-commercial software packages: *RadExPro*, Paradigm *Echos*, *OpendTect*, and *Madagascar*. Although multiple packages are not required to process HR3D data, this approach allowed the various strengths of each package to be used for generating a superior final 3D data volume. DECO's *RadExPro* was utilized for merging navigation P190 files, geometry setup, and initial data visualization. Paradigm *Echos* was introduced into the workflow for footprint removal and stacking. *Madagascar* and *OpendTect* were used for post-stack processing, the former included interpolation and post-stack migration, and the latter provided dip-steering analysis to further suppress random noise and created similarity volume for fault detection. We will discuss the key processing steps in the following section that are different from the

conventional 3D data processing. We illustrate our experience in HR3D processing and hope this can be an example workflow for similar future HR3D surveys.

2.3.1. Static corrections

The high vertical and horizontal resolution afforded by HR3D acquisition often presents significant static issues related to accurate receiver positioning and sea conditions. Meter-scale horizontal and vertical errors in position can be observed in shot gather data and mis-positioning can result in erroneous binning of data, affecting stacking and final data volume quality. In this survey, the static corrections applied include two components: a constant static time shift and a temporal tidal correction. During acquisition of the Tomakomai HR3D seismic survey, a recording delay of 4.9 ms occurred on most of the iterative (repeat) acquisition lines, which are intended for repeatability study. Thus, a constant static shift of 4.9 ms was applied to most of the acquisition lines, creating better aligned direct arrivals and reflection events. The entire acquisition was performed over a period of five days, during which the tidal levels changed vertically by up to 2 m, according to the tidal data from the Nationwide Ocean Wave Information Network for Ports and Harbours. Without having direct water velocity measurement, we consider a water velocity of 1500 m/s, a 1.5 m difference in tidal level can lead to 1 ms misalignment in a CDP gather. While small, this level of accuracy is relevant given a sampling rate of 0.25 ms, and data are improved by performing a tidal correction. Water velocity is assumed to be 1500 m/s and reflection ray paths to be zero-offset, resulting in seismic sections showing significant improvement on the alignment of recorded waveforms. Furthermore, seismic traces from each shot gather were re-sorted based on the direct arrival time and a modified offset was calculated based on the direct arrival time and water velocity. The direct arrival was automatically picked by searching the peak value within a designed window length. The modified offset further improved the waveform alignment. Specifically, after applying NMO on the CDP gathers, improved flatness was achieved using the modified offset.

2.3.2. NMO

The short (25 m) streamers in our acquisition system leads to a low-fold dataset, therefore CDP super-gathers were generated for velocity analysis. By combining the traces from 5 neighbor inline bins and 5 neighbor crossline bins, the seismic signals and velocity semblance were enhanced for velocity analysis. However, two factors have greatly impeded the velocity picking.

First, different from the hyperbolic moveout in conventional long offset seismic data, the HR3D shows almost “linear” reflection moveout. Such short offset is much less sensitive to velocity variation, thus a wide range of velocities could be the “correct” velocity. The second factor is a strong linear noise throughout our dataset, which is possibly acquisition noise, which masks the primary reflection events of interest, especially in the deeper section, which makes velocity analysis even harder.

For this survey, we eventually imported a velocity file from JGI, which was derived from their conventional 3D seismic survey undertaken just prior to the HR3D survey. We utilized velocity profiles from the overlapping region, then manually inserted one velocity function in the northern end of the HR3D survey from the super-gather velocity picks, where the 3D conventional survey does not overlap. The improved flatness suggests more accurate velocities from the conventional 3D survey, as expected.

2.3.3. F-K filtering

Strong linear noise has been observed throughout the dataset. The source is unclear, but most likely to be electrical or mechanical cable noise from the acquisition system, although significant ambient environmental noise is also present in the busy port area. Since the noise is linear, F-K filter was chosen to be the most effective method for noise suppression. Two approaches were tested to separate the noise from reflection events: Linear Moveout (LMO) and Normal Moveout (NMO).

LMO and F-K analysis suggests that the noise has two linear components with different velocities and frequencies: 200-550 Hz linear noise with 1520 m/s LMO velocity and 100-300 Hz linear noise with 2700 m/s LMO velocity. The lower velocity noise could be easily removed after applying LMO, however the higher velocity noise was mixed with the signals after LMO, thus impractical to be removed in the F-K domain.

NMO, on the other hand, flattens the reflection signals, thus separating the flat signals from the dipping noise. The dipping noise can therefore be removed in the F-K domain (Figure 6). However, the noise is inevitably mixed with signals in the lower frequency range. In order not to degrade the signals, the rejection polygon (Figure 6) was created far away from k=0, where the reflection signals align. After the application of F-K filter, the linear noise was removed and deeper signals were further boosted.

2.3.4. Interpolation

Acquisition gaps can be observed on time slices especially in the western side of the survey, where it suffers from low-fold coverage. These gaps are a result of vessel navigation in strong currents and variable sea states. In this scenario, data interpolation is required to fill in the gaps. We utilized *Madagascar* for missing data 3D interpolation (Fomel, 2002), which first estimates 3D dip along inline and crossline directions, then missing traces were interpolated using plane-wave destruction.

A total 1500 iterations were calculated for the interpolation, leading to a fully interpolated post-stack volume. Figure 7 shows examples of interpolated time slices at 42 ms and inline sections. Shapes of the gaps on the time slices suggest the acquisition lines along inline directions, therefore in certain inlines only a few traces exist, e.g. inline 1 and 2. Since the dip calculation and interpolation are performed on both inline and crossline directions, the algorithm is able to fill in such elongated gaps, leading to fully interpolated inline 1 and 2 from a few sparsely distributed traces.

2.3.5. Migration

After the application of interpolation, which corrected the irregularly and sparsely sampled data, a post-stack phase-shift migration (also known as Gazdag migration; Gazdag, 1978) was performed using *Madagascar*. Phase-shift migration is designed specifically for laterally-invariant depth migration, which extrapolates the wavefield in depth slices. Assuming a laterally homogeneous medium, the input velocity model is a single interval velocity function modified from the velocity file we obtained from JGI.

The overall stratigraphy in the Tomakomai survey area is relatively flat and the vertical velocity variation is mild, suggesting a migration may not be necessary. However, significant improvement can be observed on the time slices after the migration. Figure 8 shows an example from the shallow section (Z=55 ms). Most noticeable feature is the narrow channel on the center-right, which shows tributary systems towards the end. The width of the channel is also reduced after migration. The wide SW-NE trending band with strong amplitude contrast on the right is better outlined and enhanced. Similarly, another channel system growing from the bottom-left corner shows enhanced detail. Faint diffraction circles on the left were collapsed after the

migration. The overall footprints and random noise were also significantly suppressed, especially in the deeper section where the signal-to-noise ratio (SNR) was poor.

2.3.6. Dip-steered analysis

In order to further enhance the lateral coherence and to remove random noise, the volume was imported to *OpendTect* for dip-steering analysis. A dip-steering cube contains the local amplitude dip information at every inline and crossline position, which can be used for structurally-oriented filtering (e.g. dip-steered median filter: DSMF) and improving attributes by extracting the values along reflectors (e.g. dip-steered similarity).

In this workflow, a background steering cube was generated using BG fast steering method with a stepout of 1x1x1 (inline, crossline, and Z directions) and a median filter with a stepout of 5x5x5. The background steering cube was then used as a guidance for the generation of a DSMF volume with a stepout of 1x1. The DSMF keeps the structural features along reflectors while reducing random noise, leading to a structurally-enhanced volume which was further used for interpretation. In addition, the background steering cube and DSMF volume were further used to generate a dip-steered similarity volume, which enhanced discontinuities along reflectors for evaluation of the presence of any stratigraphic faults in the overburden.

3. Initial interpretation results

The vertical penetration depth in HR3D data depends on the source energy used and the subsurface geologic characteristics. Source power and acquisition geometry deployed during the 2017 HR3D survey allow for high-resolution imaging of the shallow subsurface down to ~600 ms (~500 meters), but signal-to-noise ratios decline significantly at greater depths, such that the injection reservoir interval at 1100 m depth is not imaged well. The final processed volume images down to 1400 ms two-way travel time (TWTT; Fig. 9), however data quality degrades below 600 ms due to the source size energy used (210 cu. in GI Gun), internal acquisition system noise, and ambient environmental noise from ship traffic in the port entrance. Conventional 3D seismic data collected in 2009 with temporary seafloor cable arrays do not image the shallow portion of the overburden with as much detail, if at all (Figure 9). This is a significant and important outcome of the HR3D acquisition, which was anticipated given prior HR3D acquisition experience in the Gulf of Mexico, but not assured given the different subsurface geology and acquisition setting.

In total eight horizons have been interpreted to date in the HR3D volume (Figure 10), including seven continuous horizons (H1 to H7, the deepest at ~360 ms) and an erosional horizon beneath H2, which is characterized by multiple channelized systems. The expected generally horizontal stratigraphy is observed, and various recognizable geological features are shown in great detail in the first 70 ms, probably representing the most recent Quaternary-Holocene relative sea level changes. Figure 10A shows a horizontal time slice at 47 ms blending amplitude and dip-steered similarity attributes for enhancing edge detection. Several erosional channels are observed at the bottom left corner (most offshore portion of dataset), and on the right side another channel with similar orientation can be seen. Strong NW-SE striking linear features with high amplitude (red-yellow; seaward dipping events) are observed in the center of the time slice are interpreted as paleo beach strand lines, commonly observed in modern coastal shore zone settings. Just to the right (northeast) of those linear features is a detached high amplitude area with lobate landward features, which are interpreted as sandy washover fans deposited during storm events. The low amplitude (blue) feature above the Xline and Inline intersection point is likely either a small incised valley or a tidal creek system. Together these features depict a paleo (Holocene?) near-offshore to onshore geomorphic transition (south to north), as would be expected at such shallow subsurface depths in this coastal setting with a slightly lower mean sea level.

Subsurface faults are often considered to be potential vertical CO_2 migration pathways, hence much effort has been put into fault detection in the HR3D data at Tomakomai. Development of a dip-steered similarity cube enhances discontinuities along reflectors on the seismic image, which has been used to interpret faults in prior similar HR3D datasets from the Gulf of Mexico (Meckel and Mulcahy, 2016). With the current data quality and processing, no significant faults are observed throughout the HR3D Tomakomai dataset using such discontinuity enhancement. The laterally continuous horizons and lack of interpreted faults provides an initial interpretation of geologically coherent overburden above the CO_2 injection site, suggesting reduced risk of vertical CO_2 migration along such features from deeper injection.

While these depositional and structural interpretations are unremarkable in many ways, there are two important points to be made with respect to HR3D applications for imaging the overburden at CCS sites: 1) the overburden is stratigraphically complex and HR3D technology allows the overburden to be understood in ways that would otherwise not be possible with existing

data (3D context; Figure 9); 2) no structural discontinuities (faults) or seismic amplitude anomalies are observed in the current dataset that would suggest any vertical migration of injected CO_2 into the overburden at the time of the survey.

4. Repeatability

Time-lapse seismic (4D seismic) surveys are a demonstrated geophysical technique to effectively monitor CO_2 injected into a saline aquifer, since seismic waves travel more slowly in CO_2-saturated sediments than water-saturated sediments, which creates significant seismic response on time-lapse data (Eiken et al., 2000; Arts et al., 2002). The ability to compare two 3D seismic surveys in time-lapse mode to detect changes occurring between surveys is largely dependent on the repeatability of the data acquired. The repeatable signal between surveys has to be consistent and larger than the non-repeatable noise (both environmental and recording system) in order to detect incremental changes between surveys, such as pore fluid changes (i.e. brine to CO_2).

During the acquisition of Tomakomai HR3D survey, 60% of the sail lines were repeated (the iterative pass) a few days after the initial acquisition of these lines (the primary pass). Iterative passes were acquired in order to preliminarily inform repeatability of the HR3D technology, as well as to increase data coverage and signal-to-noise ratio directly above the CO_2 injection location. Ideally, when acquiring iterative passes of the same sail line, the shot and receiver locations are intended to be in identical locations. Pragmatically, this cannot be achieved due to variable sea conditions and their effect on array geometry and vessel position and navigation. Figure 11 shows an example of a single shot geometry (source and receiver locations) of the primary and iterative passes of the same intended sail line, illustrating the overall similarity (short physical separation) of the shot geometry from two passes which were acquired three days apart. Overall, similar comparisons of shot records from nearly identical shot locations, but separated in time by days, show very good qualitative pre-stack repeatability.

In this preliminary repeatability evaluation, the data from all the iterative and primary passes were separated and processed into two individual stacked volumes using the same processing workflow and parameters previously described in Section 2. Figure 12 presents the same inline section extracted from the two volumes, and their raw amplitude spectra. While the

differences in the vertical gaps in the sections is a result of the binning of the data and the position of the shot and receiver locations in two passes, similar amplitude characteristics (location, continuity, magnitude) of the datasets can be visually observed. This is the expected outcome, although visual qualitative comparison is not the most rigorous way to demonstrate repeatability (Waage et al., 2018). For the Tomakomai CO_2 storage project, a second (time-lapse) HR3D acquisition comvering a similar footprint is currently planned for 2019, and more detailed quantitative repeatability analyses such as normalized RMS difference (NRMS; Grion et al., 2000; Kragh and Christie, 2002) and measurement of predictability (Kragh and Christie, 2002; White, 1980) will be performed in the following studies. In addition, the source size will be doubled in order to image deeper interval and improve the overall SNR. More accurate positioning methodology will be deployed to tackle static issues encountered during HR3D data processing.

In summary, our preliminary repeatability study shows encouraging potential for a planned future 4D survey. More detailed repeatability analysis will be conducted once the 4D survey is acquired. The ability for HR3D to detect potential CO_2 leakage in the overburden above CO_2 inject sites suggests HR3D technology can be a very effective monitoring tool.

5. Conclusions

This study demonstrates the first successful acquisition, processing, and interpretation of shallow marine HR3D seismic data acquired over an active offshore CO_2 injection site. Sensitivity analysis conducted prior to acquisition indicated favorable subsurface conditions for observing a seismic response related to changes in pore fluids, further motivating HR3D acquisition. A unique processing workflow incorporating multiple data processing software packages has been tailored to the short-offset and low-fold HR3D acquisition. The final 3D volume shows complex shallow geology but generally sub-horizontal and continuous stratigraphy in the overburden above the injection zone without identifiable faults, which indicates geologically coherent overburden above the CO_2 injection site. Although continuous stratigraphy in the overburden is not indicative of zero migration risk, the absence of steeply dipping faults throughout the dataset suggests reduced risk of vertical migration. Moreover, no “chimney” features are observed in the HR3D volume, suggesting no vertical migration of injected CO_2 at the time of the survey. Initial investigations into repeatability suggest potential for favorable repeatability between 3D surveys (4D analysis) for the overburden interval, but has yet to be demonstrated by an actual repeat survey, suggesting

that HR3D technology may be a very effective time-lapse monitoring tool in the overburden above CO_2 injection sites, although more formal quantitative evaluation is deferred until a second HR3D acquisition, planned for 2020. Although the current CO_2 injection at Tomakomai site is at ~100 KT scale, the successful deployment of this novel marine seismic technology validates HR3D to be an appropriate and useful characterization and monitoring tool for the overburden at large-demonstration and commercial-scale offshore CCS sites as well.

Acknowledgements

The authors appreciate the Japan Ministry of Economy, Trade and Industry and Japan CCS Co., Ltd. for providing the opportunity to acquire HR3D data at the Tomakomai CCS site. The authors also thank JGI, Inc. for collaboration, mobilization, and providing GPS locations of sources and receivers for the HR3D acquisition. Dr. Meckel is especially grateful to Yutaka Tanaka at JCCS for his excellent assistance with implementing the HR3D project, a first of its kind for CCS. We are grateful to the JGI crew involved in marine seismic acquisition, especially Shigeyuki Suda and his superb technical team. This material is based upon work supported by the U.S. Department of Energy – National Energy Technology Laboratory, under award agreement DE-FE0028193 DOE-Validation of MVA Tools for Offshore CCS: Novel Ultra-High-Resolution 3D Marine Seismic Technology (P-Cable).

References

Arts, R., R. Elsayed, L. van der Meer, O. Eiken, S. Ostmo, and A. Chadwick, 2002, Estimation of the mass of injected CO_2 at Sleipner using time-lapse seismic data. 64th European Association of Geoscientists and Engineers (EAGE) Meeting, Florence, Paper H016, p. 4

Batzle, M. and Wang, Z., 1992, Seismic properties of pore fluids, Geophyics Vol. 57, No.11, p.1396-1408.

Brookshire, B.N., C. Lippus, A. Parish, B. Mattox, and A. Burks, 2016, Dense arrays of short streamers for ultrahigh-resolution 3D seismic imaging, The Leading Edge, July 2016: 594-599, http://dx.doi.org/10.1190/tle35070594.1.

Cerveny, V., and J.E.P. Soares, 1992, Fresnel Volume Ray Tracing, Geophysics 57(7).

Eiken, O., Brevik, I., Arts. R., Lindeberg, E., & Fagervik, K., 2000, Seismic monitoring of CO_2 injected into a marine aquifer. SEG Calgary 2000 International conference and 70th Annual meeting, Calgary, paper RC-8.2.

Fomel, S., 2002, Applications of plane-wave destruction filters: Geophysics, 67, 1946–1960, https://doi.org/10.1190/1.1527095.

Gassmann, F., 1951, On the elasticity of porous media, Veirteljahrsschrift der Naturforschenden Gesellschaft in Zurich, 96, 1-23.

Gazdag, J., 1978, Wave equation migration with the phase-shift method: Geophysics, 43, 1342-1351.

Grion, S., J. Keggin, S. Ronen, and J. Caldwell, 2000, Seismic Repeatability Benchmarks. Offshore Technology Conference. doi:10.4043/12099-MS

Han D.H., Sun, M., and Batzle, M., 2010, CO2 velocity measurement and models for temperatures up to 200°C and pressures up to 100 MPa, Geophysics, Vol.75, No.3, P E123-E129.

Hashin, Z. and Shtrikman, S. 1963 - A variational approach to the theory of the elastic behaviour of multiphase materials, Journal of the Mechanics and Physics of Solids, Vol.11, issue 2, p. 127-140.

Ikeda, T., and T. Tsuji, 2015, Advanced surface-wave analysis for 3D ocean bottom cable data to detect localized heterogeneity in shallow geological formation of a CO_2 storage site, IJGGC, 39: 107-118.

Ito, D., Matsuura, T., Kamon, M. Kawada, K., Nishimura, M., Tomita, S., Katoh, A. Akaku, K., Inamori, T., Yamanouchi, Y., Mikami, J., 2013, Reservoir evaluation for the Moebetsu Formation at Tomakomai candidate site for CCS demonstration project in Japan, Energy Procedia, No. 37, 4937-4945.

Kragh, E. and P. Christie (2002). Seismic repeatability, normalized rms, and predictability. The Leading Edge, 21(7), 640-647.

Lebedeva-Ivanova, N., S. Polteau, B. Bellwald, S. Planke, C. Berndt, and H.H. Stokke, 2018, Toward one-meter resolution in 3D seismic, The Leading Edge, November, 818-828, https://doi.org/10.1190/tle37110818.1.

Lumley, D., 2010, 4D seismic monitoring of CO_2 sequestration, The Leading Edge, February, p. 150-155.

Mavko, G., Dvorkin, J., Mukerji, T., 2003, The Rock Physics Handbook, Cambridge University Press.

Meckel, T.A., and F.J. Mulcahy, 2016, Use of novel high-resolution 3D marine seismic technology to evaluate Quaternary fluvial valley development and geologic controls on shallow gas distribution, inner shelf, Gulf of Mexico, Interpretation, 4(1): SC35-SC49, http://dx.doi.org/10.1190/INT-2015-0092.1.

Reuss A., 1929, Berechnung der Fliessgrenzen von Mischkristallen auf Grund der Plastizitatsbedingung fur Einkristalle, Zeitschrift fur Angewandte Mathematik und Mechanick, 9, 49-58.

Smith, T.M., C.H. Sondergeld, and C.S. Rai, 2003, Gassman fluid substitutions: a tutorial, Geophysics, 68(2): 430-440.

Sugihara, M., Y. Nishi, H. Ikeda, K. Nawa, and T. Ishido, 2017, Monitoring CO_2 injection at the Tomakomai field using high-sensitivity continuous gravimetry, Energy Procedia, 114: 4020-4027.

Tanaka, Y., Masanori Abe, Yoshihiro Sawada, Daiji Tanase, Toshikazu Ito, Tetsuo Kasukawa, 2014, Tomakomai CCS Demonstration Project in Japan, 2014 Update, Proceedings of GHGT-12, Energy Procedia 63 (2014) p. 6111 – 6119.

Tanaka, Y., Y. Sawada, D. Tanase, J. Tanaka, S. Shiomi, T. Kasukawa, 2017, Tomakomai CCS demonstration project of Japan, injection in process, Energy Procedia, 114:5836-5846.

Tanase, D. and Y. Tanaka, 2019, Progress of CO_2 injection of the Tomakomai CCS demonstration project, GHGT-14.

Vera, V.C., and D.C. Lawton, 2010, Fluid substitution and seismic modelling in a sandstone aquifer, CREWES Research Report, v. 22, 29 pp.

Waage, M., S. Bunz, M. Landro, A. Plaza-Faverola, and K. Waghorn, 2018, Repeatability of high-resolution 3D seismic data, Geophysics, https://doi.org/10.1190/geo2018-0099.1

White, R., 1980, Partial coherence matching of synthetic seismograms with seismic traces. Geophysical Prospecting, 28: 333-358. doi:10.1111/j.1365-2478.1980.tb01230.x

Xue, Z., and T. Ohsumi, 2004, Seismic wave monitoring of CO_2 migration in water-saturated porous sandstone, Exploration Geophysics, 35, 25–32.

480 **FIGURES**

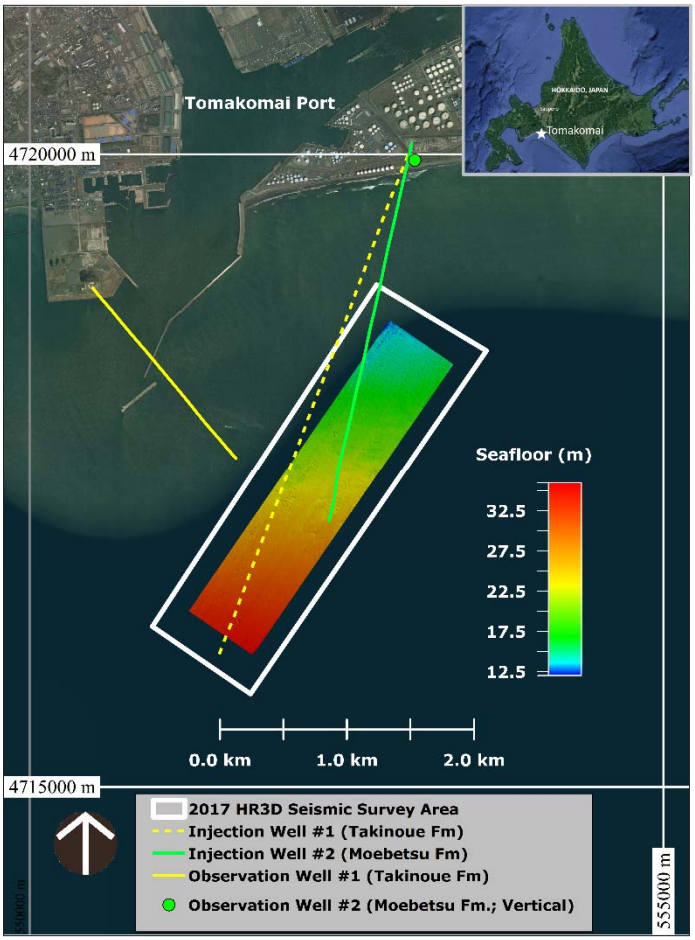

481

482 Figure 1: Location of the August 2017 HR3D seismic survey collected as a collaboration
483 between JGI and the GCCC at The University of Texas at Austin. Seafloor depth based on
484 HR3D seismic data collected. UTM grid lines. Inset map of Hokkaido in upper right.

485

V_P (m/s)	V_S (m/s)	Bulk density (kg/m^3)	Porosity (%)	Kmin (GPa)
2030	593	1813	28	40.9

Temperature = 44.8 C **Pore Pressure** = 10.67 MPa	**Bulk modulus (GPa)**	**Density (kg/m^3)**
Brine	2.49	1007
CO_2	0.0038	265

Table 1: Moebetsu average properties derived from well-log data and core analysis. In-situ temperature and pressure (Han et al, 2010) are used to derive bulk modulus and density for brine and CO_2.

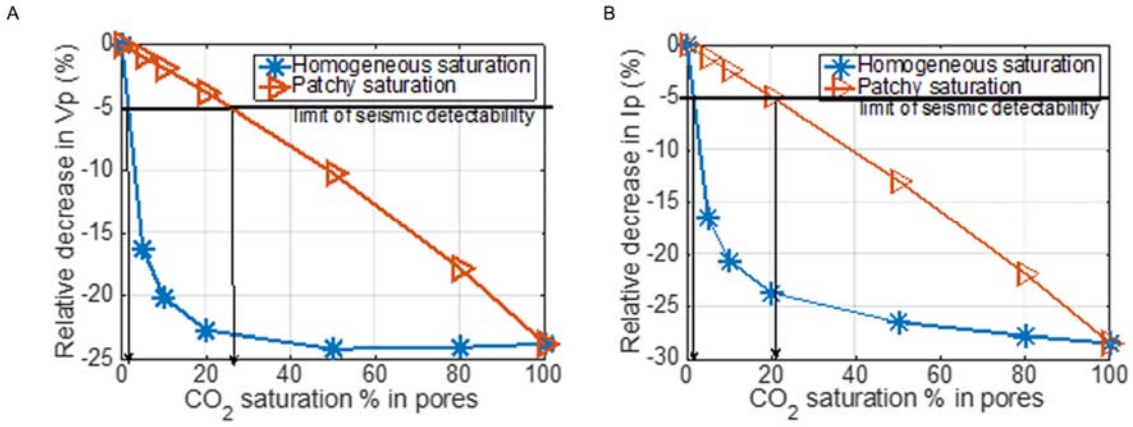

490

491 Figure 2: Calculated relative (%) decrease in P-wave velocity (Vp, left) and Acoustic Impedance
492 (Ip, right) as a function of CO_2 saturation in pores for homogeneous saturation and patchy
493 saturation assumptions. Superimposed on the figure is a line at -5% decrease, taken as a
494 conservative limit of seismic detectability at the site.

495

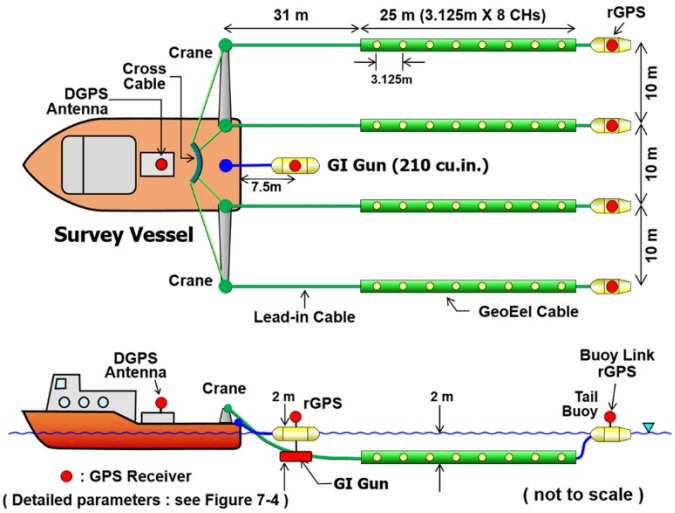

496

497 Figure 3: The HR3D seismic acquisition geometry. Image courtesy of JGI.

498

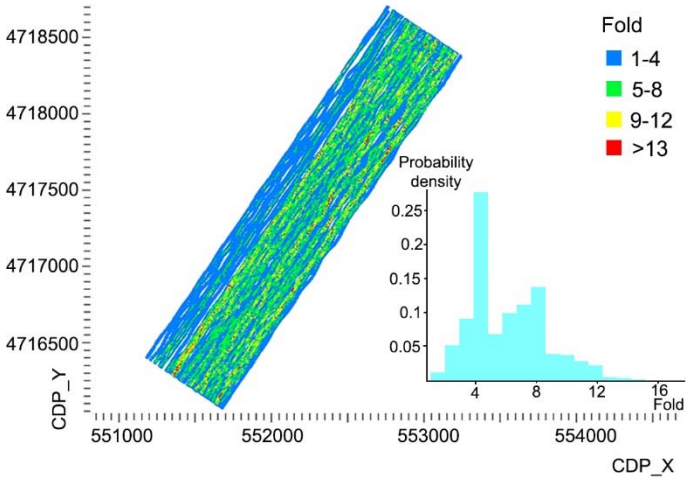

Figure 4: Fold map of common depth points (CDP) for the 2017 HR3D survey. Higher fold exists on the eastern side of the survey area due to higher number of iterative (repeat) line acquisition.

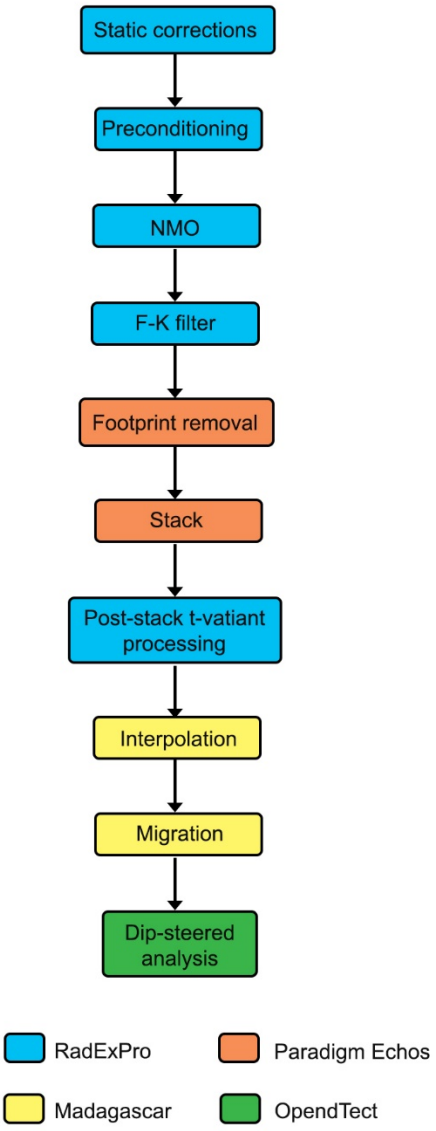

504

505 Figure 5: The HR3D seismic data processing workflow. Colors indicate different processing
506 software used in the workflow. See text for processing details.

507

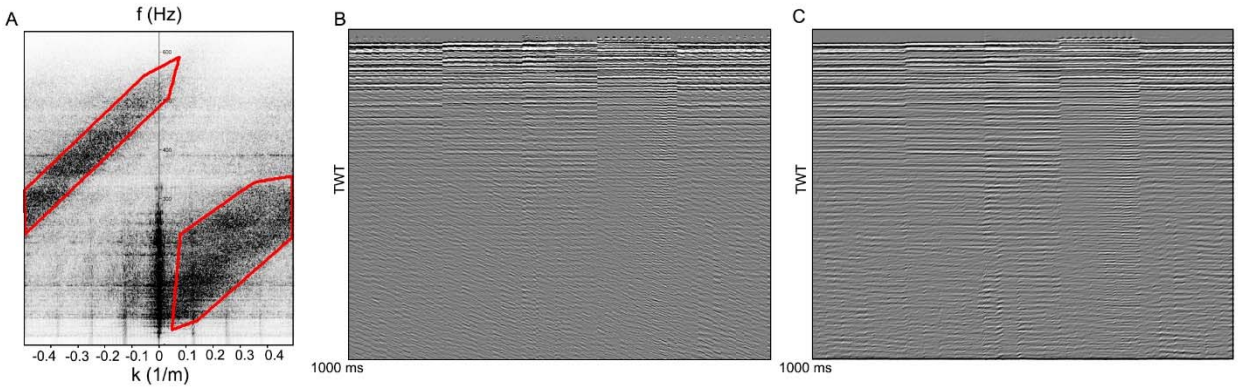

508

509 Figure 6: F-K filter used for linear noise removal. A) F-K filter and rejection polygon (in red).
510 NMO-corrected shot gathers before and after applying the FK filter are shown in (B) and (C),
511 respectively. Note the linear noise does not decay with noise, suggesting it is an acquisition
512 noise.

513

514

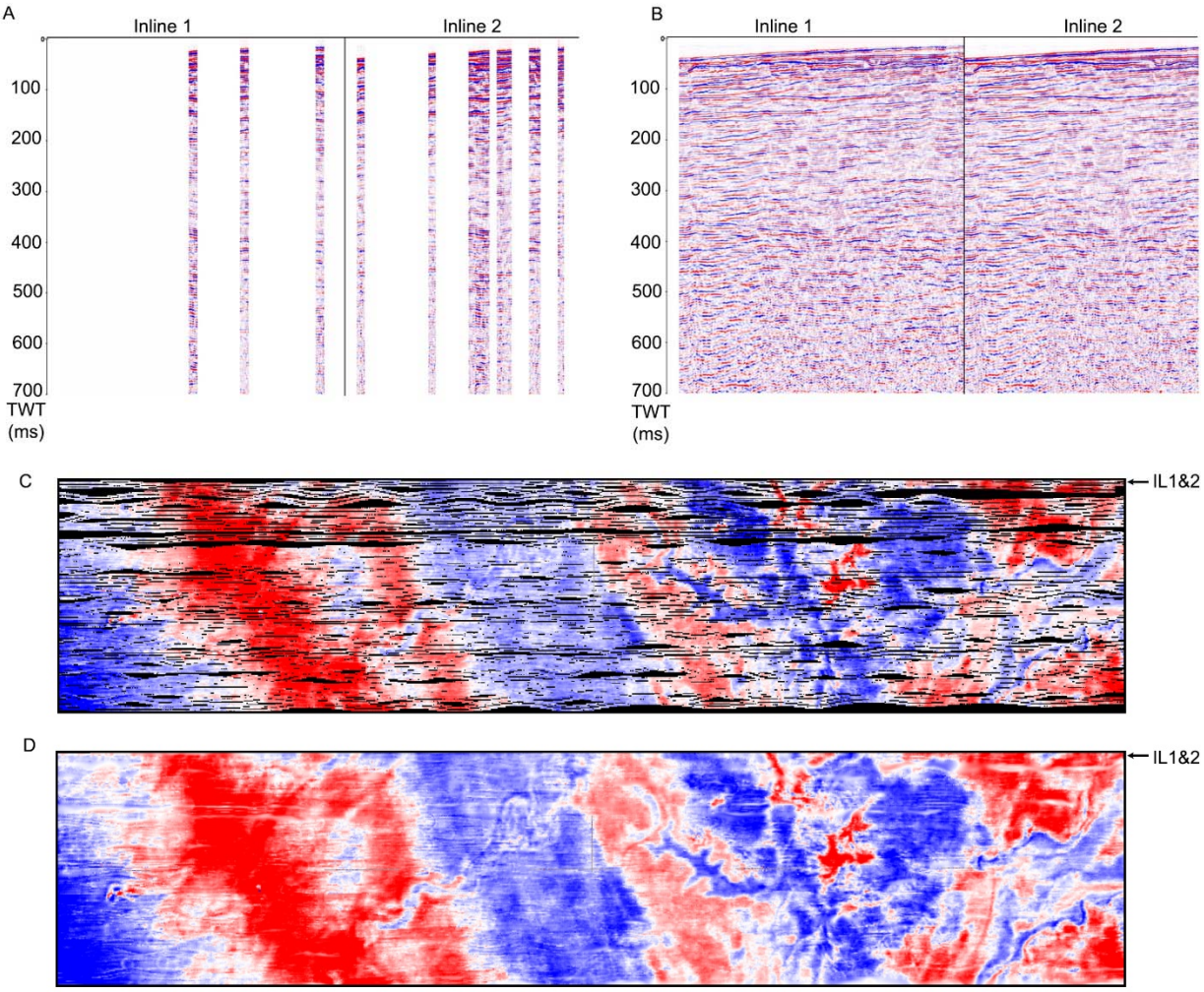

515

516 Figure 7: Comparison of before (A & C) and after (B & D) the application of interpolation in inline
517 section and time slice (Z=42 ms). The location of the inline 1 and 2 is labeled as arrows in C & D.

518

519

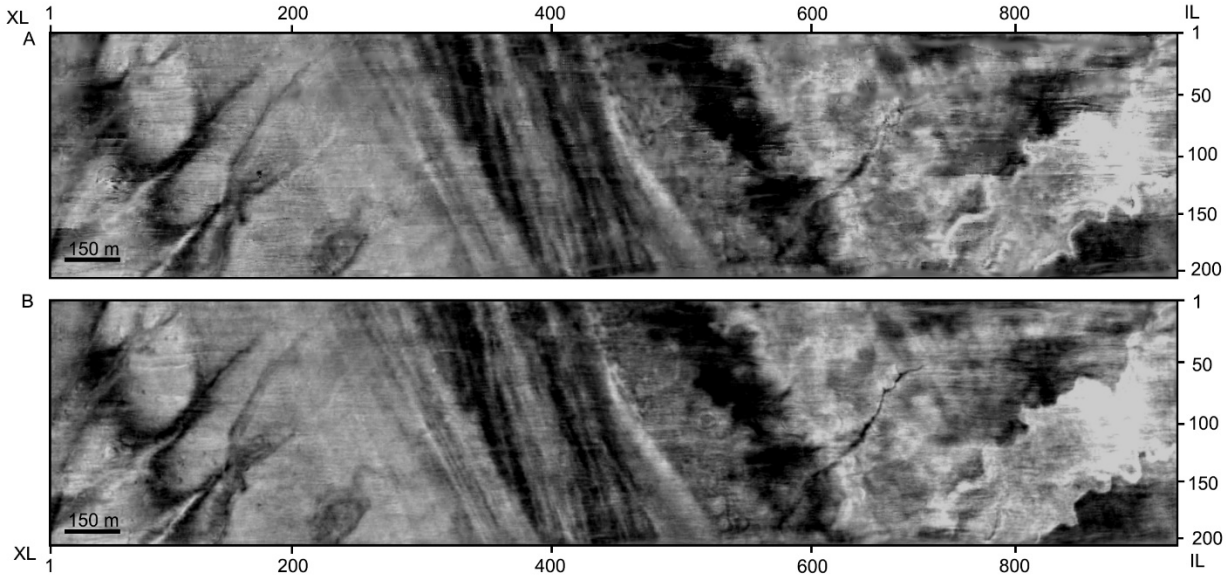

520

521 Figure 8: A time slice at Z=55 ms showing the difference from before (A) and after (B) applying
522 a post-stack phase-shift migration. Note feature margin sharpening. Footprint of the time slice is
523 shown in Figure 1. See Figure 10 for color version.

524

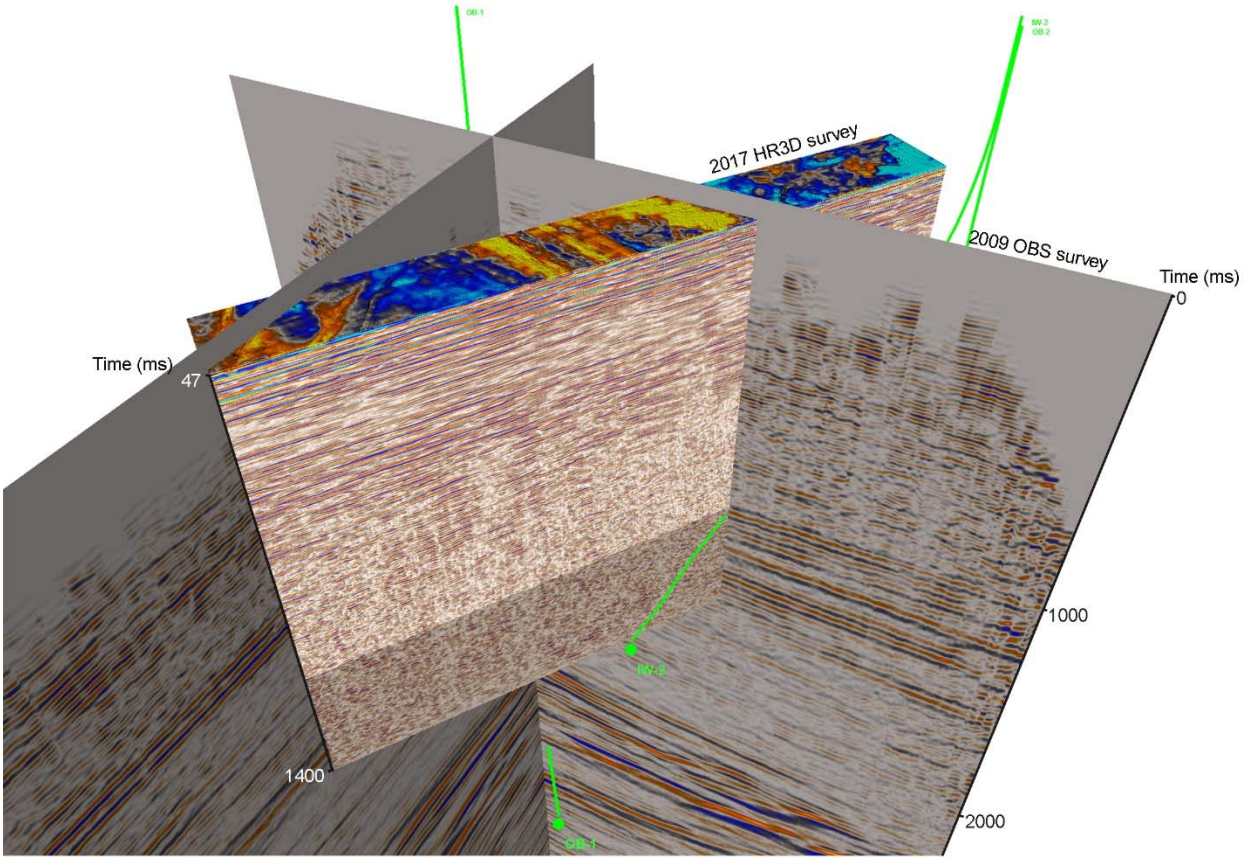

Figure 9: Integration of conventional and HR3D seismic data for the Tomakomai site. HR3D data provide more continuous coverage and higher horizontal and vertical data resolution in the interval above the injection interval (labeled IW-2) than the conventional 3D ocean bottom seismic (OBS) data acquired with temporary seafloor cable array (2D slices shown).

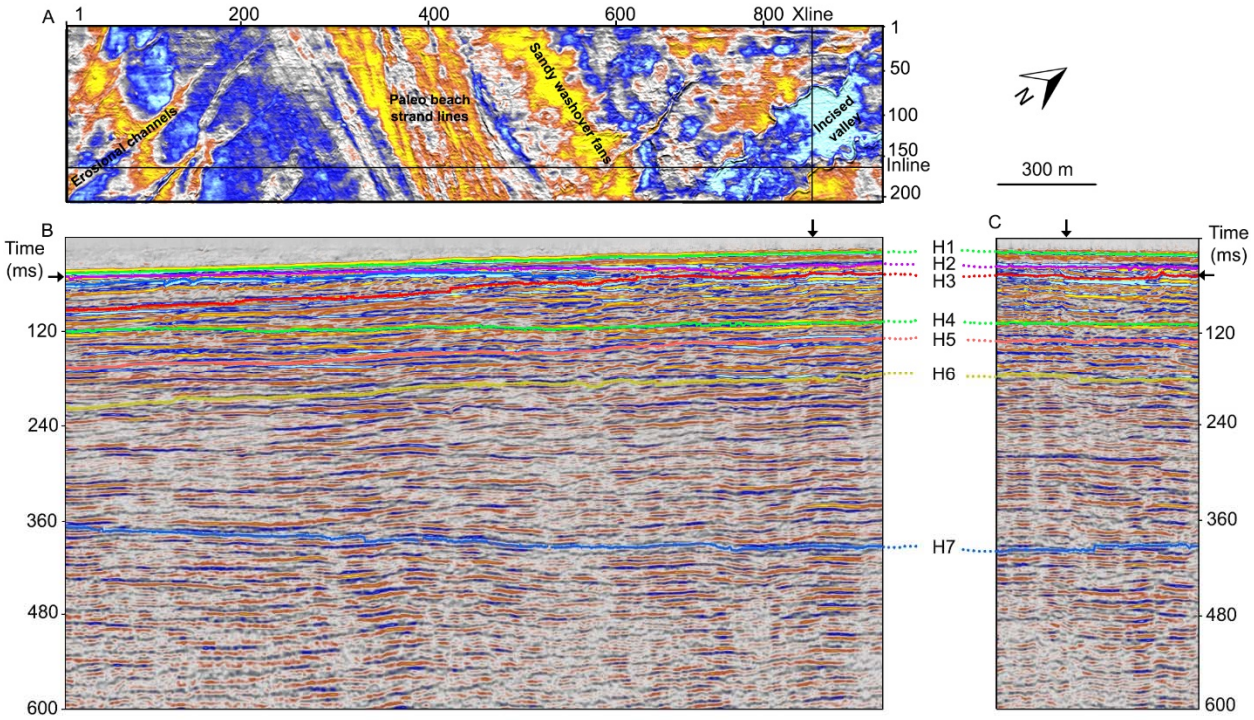

Figure 10: Initial processed volume and interpretation of the HR3D seismic. Figure record length in B is 600 msec TWTT, or approximately 550 m depth below sea surface. Horizontal arrow symbol on left side of inline section B denotes the location of the time slice (A) at 47 ms. Downward pointed arrows symbols at top of inline (B) and crossline (C) section indicate intersections as shown in A. See Fig. 1 for depth map of H1 surface.

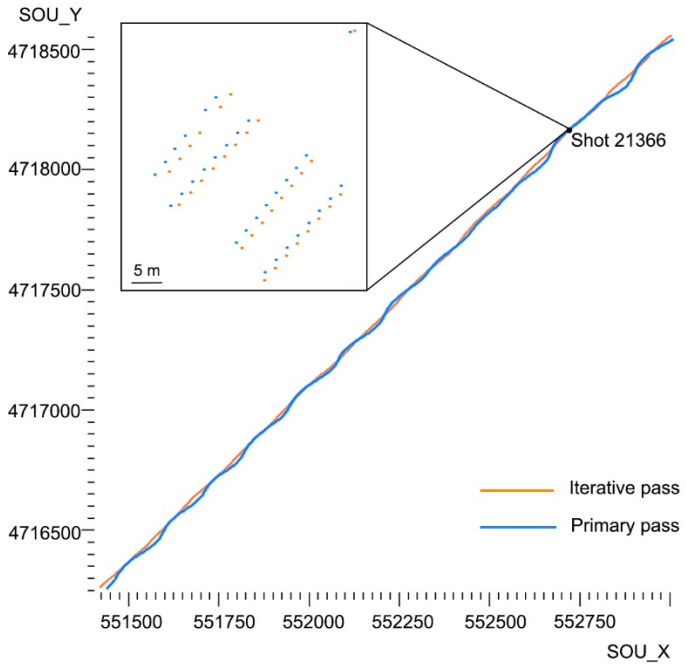

538

539 Figure 11: Shot source-receiver geometry of the primary and iterative passes of the same sail
540 line. Axes are in UTM meters. Inset: geometry of arbitrary shot 21366 source and receiver
541 positions from the two passes (note 5 m scale bar). For many instances, the maximum difference
542 of the distance between analogous shots and receiver positions for primary and iterative passes is
543 less than 3 m (i.e. the bin size).

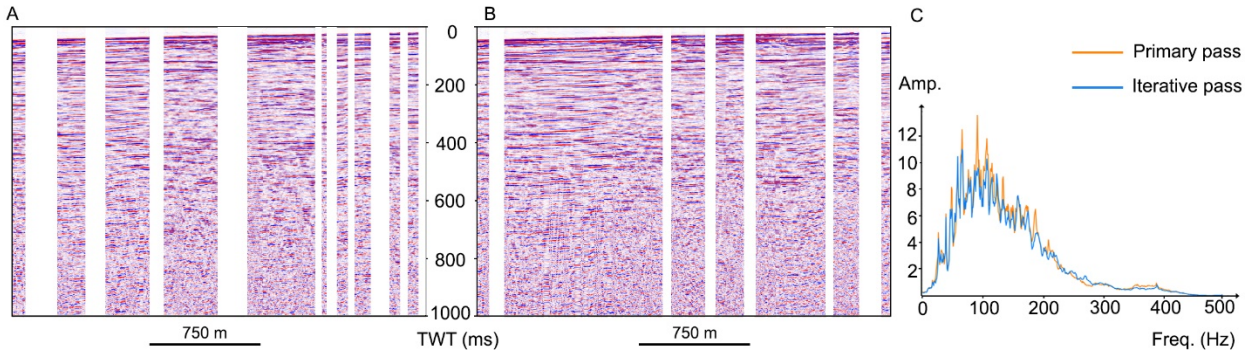

Figure 12: Inline comparison between separate stacked volumes of 2017 HR3D data using A) primary passes and B) iterative passes, and their C) raw amplitude spectra. The same bin geometry is used for both stacked volumes, resulting in data gaps from variable CDPs from imperfect shot receiver location replication. These results suggest that time-lapse analysis comparing two HR3D volumes will be valuable, and a second HR3D survey is planned for a similar footprint in 2019.